

Magnetic resonance spectroscopy metabolic profiling reveals different mechanisms of action in response to signaling inhibitors in prostate cancer

A. Lodi¹, and S. M. Ronen¹

¹University of California San Francisco, San Francisco, California, United States

Introduction. Deregulation of the phosphatidylinositol 3-kinase (PI3K) and mitogen-activated protein kinase (MAPK) signaling pathways is observed in many human cancers, and inhibitors of these pathways are under investigation as targeted anticancer treatments. LNCaP and PC3 cell lines are two extensively studied models of early stage androgen-dependent and advanced androgen-independent human prostate cancer, respectively. In both these cell models, PI3K is activated due to PTEN deficiency. The goal of this study was to assess the value of an untargeted, ¹H magnetic resonance spectroscopy (MRS)-based metabolomics approach to assess the effects of treatment with inhibitors of the PI3K and/or MAPK pathways and evaluate possible candidate metabolites as biomarkers of signaling inhibition.

Methods. LNCaP and PC3 prostate cancer cells were treated for 48 hours with LY294002, an inhibitor of the PI3K pathway, and 17AAG, a geldanamycin-analogue which induces the simultaneous inhibition of the MAPK and PI3K pathways by targeting the heat-shock protein 90 (HSP90). Following treatment, the cells were extracted using a dual phase extraction and the dried polar extracts were redissolved in 90% H₂O/10% D₂O phosphate buffer (pH 7). 1D ¹H MRS data were acquired at 600 MHz using a 90° pulse, 4 s relaxation delay and 8 kHz spectral width. The water signal was suppressed using excitation sculpting. The full MRS datasets acquired on the LNCaP and PC3 intracellular extracts (8 replicates per treatment condition per cell lines) were then analyzed using principal component analysis (PCA).

Results. For both cell lines, the scores plots obtained from the PCA (Fig. a and b representing PC3 and LNCaP, respectively) were characterized by tight grouping within each treatment and complete separation between the control and each of the two treatment groups. The first principal component (PC1), recapitulated about 46% and 50% (for PC3 and LNCaP cells, respectively) of the variability and separated the control and 17AAG-treated groups from the LY294002 treatment. Complete separation among the treatment groups is also observed along PC2 (about 30% variability). To gain a better understanding of the metabolic changes underlying the observed differences we then performed pair-wise PCAs comparing the solvent control to each of the drug treatments. As expected, PC1 captures most of the variability for all these analyses (e.g. Fig. c). Close inspection of the PC1 loadings plots (e.g. Fig. d for PC3 cells) obtained from the pair-wise analyses allows identification of the specific metabolites responsible for the separation. For instance phosphocholine is depleted to 51±4% (p=0.00001) and 87±4% (p=0.0002) of control in PC3 and LNCaP cells following treatment with LY294002 and accumulates to 147±12% (p=0.00001) and 110±5% (p=0.002) of control in PC3 and LNCaP cells following treatment with 17AAG. These results recapitulated previous observations in human breast cancer cell lines (1,2). We also observed decreased intracellular lactate levels in both cell lines and with both drug treatments (61±8% (p=0.00002) and 79±10% (p=0.001) of control for LY294002 and 17AAG treatments in PC3 cells and 69±11% (p=0.002) and 83±13% (p=0.04) of control for LY294002 and 17AAG treatments in LNCaP cells). The loadings plots also indicate the presence of additional common metabolic changes across both treatments and cell lines, such as the accumulation of several amino acids (e.g. branched amino acids). Importantly, this method also identified citrate as a previously unreported, key metabolic change in prostate cells treated with 17AAG. Reduced citrate has been previously proposed as a biomarker of malignant transformation in prostate due to a marked decrease in the concentration of this metabolite in prostate cancer (3). Following 17AAG treatment, citrate is the most prominent discriminant metabolite for 17AAG-treated PC3 cells and is detected in treated but not in control cells (Fig. e). A similar outcome was also observed in 17AAG-treated LNCaP cells, though to a lesser extent since these cells represent a less advanced cancer and, unlike PC3, have detectable basal levels of citrate.

Discussion and Conclusion. Regulation of the PI3K/Akt pathway has been previously shown to contribute to modulation of cell metabolism (4). Here we have investigated the effect on cell metabolism of LY294002, a PI3K inhibitor, and 17AAG, a combined PI3K/MAPK inhibitor. Several common metabolic consequences of these drug treatments were observed across different cell lines and indicate that these metabolites, in particular lactate, could represent biomarkers of response to PI3K inhibitor treatment. Finally, of great interest in the context of prostate cancer is the observation that 17AAG is able to induce a significant increase in citrate accumulation. This work highlights the value of an untargeted metabolomics approach for identifying metabolic changes that can inform on drug mechanism of action and potentially serve as biomarkers of drug action. Further studies are needed to fully understand the underlying mechanisms inducing these effects on cell metabolism.

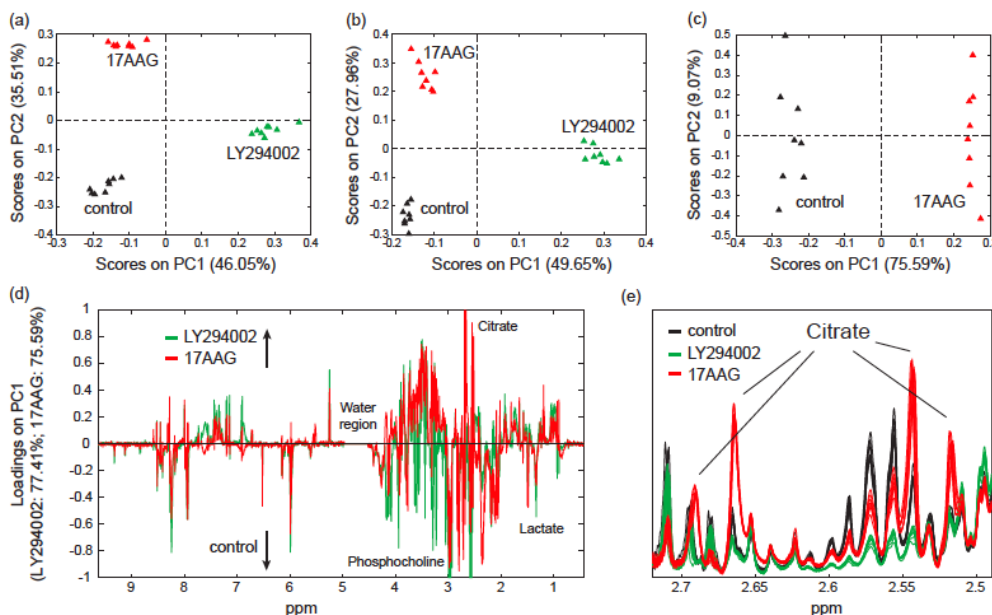


Figure 1. Scores plots obtained from the principal component analysis (PCA) of the full ¹H MRS datasets acquired on (a) PC3 and (b) LNCaP cell extracts after treatment with LY294002 or 17AAG. (c) Scores plot from the pair-wise PCA comparing only control and 17AAG-treated PC3 cells. Loadings plot obtained from the pair-wise PCA on (d) PC3 treated with either LY294002 or 17AAG (e) LNCaP.

References:

- 1 Beloueche-Babari M et al., Mol Cancer Ther, 2006;5(1):187-96.
- 2 Brandes AH et al., Breast Cancer Res, 2010;12(5):R84.
- 3 Kurhanewicz J et al., Urology, 1995;45:459-467.
- 4 Elstrom RL et al., Cancer Res, 2004;64(11):3892-3899.

Acknowledgements: This work was supported by NIH grant RO1 CA130819.